Available online at www.sciencedirect.com
ScienceDirect
ELSEVIER
Computer Communications xxx (2007) xxx–xxx
computer communications
www.elsevier.com/locate/comcom

QoS and energy efficiency in network wide broadcasting: A MAC layer perspective

Bulent Tavli [a,*], Wendi B. Heinzelman [b]

[a] *TOBB University of Economics and Technology, Computer Engineering Department, 06560 Ankara, Turkey*
[b] *University of Rochester, Department of Electrical and Computer Engineering, Rochester, NY 14627, USA*

Received 5 February 2007; received in revised form 6 July 2007; accepted 28 July 2007

Abstract

In this paper we investigate the role of medium access control on the performance of network-wide real-time data broadcasting through flooding using three MAC protocols (IEEE 802.11, CPS, and MH-TRACE) in terms of QoS (packet delivery ratio, packet delay, and delay jitter) and energy dissipation. We conduct extensive simulations to evaluate the performance of network-wide broadcasting through flooding in the node density, traffic load, and network size/topology parameter space. The results of our study show that different MAC protocols produce better performance than the others in different parts of the parameter space. Thus, in designing network layer broadcast architectures, the characteristics of the medium access control layer should be given the utmost importance to ensure the satisfactory performance of the system.

Keywords: Protocols; Multi-access communication; Energy efficiency; Speech communication; Quality of Service (QoS); Real-time systems

1. Introduction

In many applications, one of the most important functions of a mobile ad-hoc radio network is to create a platform for voice communications. Due to the limited radio range, single hop broadcasting to all the nodes in the network is not possible in many ad hoc network scenarios, and thus multi-hop broadcasting is unavoidable.

In network-wide voice broadcasting there are three main criteria to evaluate the performance of the network architecture: application quality of Service (QoS), energy efficiency, and efficient spatial reuse. QoS for voice communications requires that (i) the maximum packet delay is kept within specific bounds, (ii) the packet delivery ratio is kept above the minimum requirements of the application, and (iii) delay jitter is low [1–8]. Note that the QoS of voice communications is affected by many other criteria, such as echo and noise; however, from a networking perspective, packet delivery ratio, packet delay, and delay jitter are the main metrics to evaluate voice QoS.

Energy efficiency is crucial to support short-range lightweight radios operating with limited energy. Avoiding energy waste for these radios is of the utmost importance in order to keep the nodes connected to the network [9,10]. The final QoS parameter, spatial reuse, is related to the number of simultaneous rebroadcasts and is required for bandwidth efficiency. Since in this study we focus on the medium access control layer, we do not address spatial reuse efficiency, which is mostly related with the network layer.

Characterizing the effects of medium access control on the behavior of network-wide broadcasting is essential for designing high performance broadcasting architectures (network layer and MAC layer). We utilize flooding as our network layer broadcast algorithm due to its simplicity, which makes the role of the MAC layer more transparent and observable than more complicated broadcast algorithms.

* Corresponding author. Tel.: +90 312 292 4074; fax: +90 312 292 4180.
E-mail address: btavli@etu.edu.tr (B. Tavli).

0140-3664/$ - see front matter © 2007 Elsevier B.V. All rights reserved.
doi:10.1016/j.comcom.2007.07.005

Please cite this article in press as: B. Tavli, W.B. Heinzelman, QoS and energy efficiency in network wide broadcasting: ..., Comput. Commun. (2007), doi:10.1016/j.comcom.2007.07.005

In this study, we investigate and quantify the QoS and energy dissipation characteristics of flooding when it is used for real-time data broadcasting for three different MAC protocols through extensive simulations and in depth analysis. We believe that the results of this study are a valuable contribution to the better understanding of QoS and energy efficiency for network-wide broadcasting.

1.1. QoS

In broadcasting scenarios, where acknowledged data delivery is not practical, QoS of streaming media is determined primarily by the MAC layer. QoS for streaming media throughout the network necessitates timely delivery of packets (bounded delay), high packet delivery ratio, and low jitter. Packet delay is directly related with the number of hops traversed by the voice packets and the congestion level of the network. In a highly congested network, the packets are backlogged in the MAC layer before they can be transmitted, which increases the packet delay beyond the acceptable limits. To ease congestion, packets that have exceeded the delay bound can be dropped rather than transmitting them to the destination, as they are no longer useful to the application. However, excessive packet drops decrease the packet delivery ratio, which is the other important aspect of QoS for streaming media. Packet delivery ratio is also decreased by collisions. Thus, there are two mechanisms that negatively affect the packet delivery ratio: packet drops and collisions.

The overall deterioration of QoS in voice communications can be expressed as the sum of individual factors, such as packet delay, packet loss, jitter, noise, and echo [3–6]. Furthermore, the net effect of the distortion depends also on the codec specifications and the voice coding scheme utilized. In this study, we focus our attention on the effects of packet delay and packet drops on QoS; however, we also kept track of the delay jitter. In this study, the QoS objectives are 95% packet delivery ratio and 150 ms maximum packet delay. Voice packets exceeding 150 ms delay are dropped at the MAC layer (*i.e.*, $T_{\text{drop}} = 150$ ms). Thus, the resulting utility function uses a hard constraint satisfaction scheme, where either the QoS is satisfied or not (see Fig. 1) [11]. Although the utility function presented in Fig. 1 is a rather simplified version of an actual utility function with higher dimensionality, we believe it satisfactorily captures the essence of the actual model for evaluating the QoS performance of network-wide voice broadcasting.

1.2. Energy dissipation

Avoiding energy waste is crucial in order to keep the nodes connected to the network. The energy dissipation modes of a radio can be organized into five categories: (i) transmit mode, (ii) receive mode, (iii) idle mode, (iv) carrier sense mode, and (v) sleep mode. Transmit energy is dissipated for packet transmissions. Receive energy is dissipated on receiving packets from a node located in the transmit range (see Fig. 2). Carrier sense energy dissipation is similar to receive energy dissipation [12], but in carrier sensing the source node is located in the carrier sense region rather than the transmit region. Idle energy dissipation is the energy dissipated when none of the nodes in the transmit range and carrier sense range are transmitting packets and the receiving node is not in the sleep mode. Sleep mode energy is dissipated on electronic circuitry to keep the radio in a low energy state that can return back to active mode in reasonable time, when required.

To illustrate the energy dissipation characteristics of a simple network wide broadcasting architecture (flooding using the IEEE 802.11 MAC), we present an example scenario. Fig. 3 shows the relative amount of energy dissipation per node in the transmit, receive, carrier sense, and idle modes for an 800 by 800 m area network with 40 nodes and a source sending data at 32 Kbps. Further details of this scenario can be found in Section 4. The largest component of energy dissipation is carrier sensing (44.9%), which is followed by receive energy dissipation (31.2%) and idle energy dissipation (19.3%). Transmit energy dissipation (4.7%) is the smallest component of the total energy dissipation. Since the underlying medium access control (MAC) protocol, which is IEEE 802.11, does not support a n efficient low-energy sleep mode in ad hoc (infrastructureless) mode, energy dissipated in the sleep mode is zero.

In a typical energy model, sleep mode energy dissipation is significantly lower than the other energy dissipation modes [9] (see Fig. 4). Energy-efficient distributed protocol design can be described as creating an appropriate distributed coordination scheme that minimizes a radio's total energy dissipation without sacrificing its functionality, by

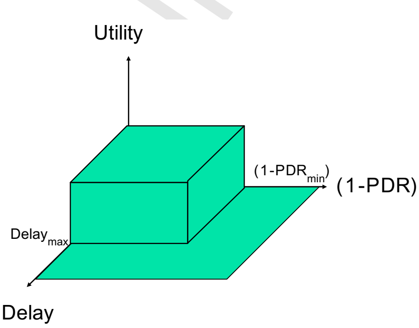

Fig. 1. Delay-Packet Delivery Ratio (PDR) utility function.

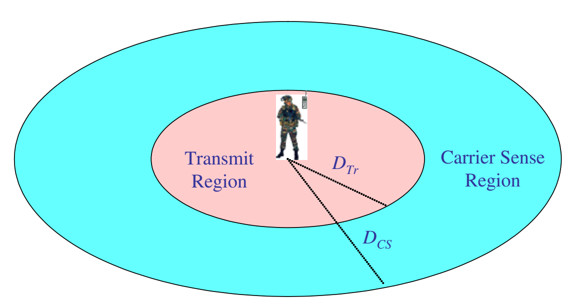

Fig. 2. Illustration of transmit and carrier sense regions.

Please cite this article in press as: B. Tavli, W.B. Heinzelman, QoS and energy efficiency in network wide broadcasting: ..., Comput. Commun. (2007), doi:10.1016/j.comcom.2007.07.005

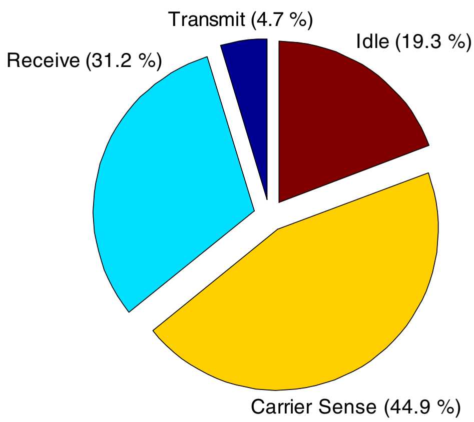

Fig. 3. Energy dissipated on transmit, receive, idle, and carrier sense modes for flooding with IEEE 802.11 in an 800×800 m network with 40 nodes.

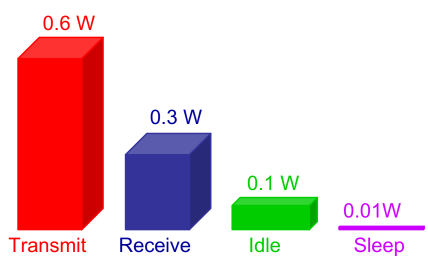

Fig. 4. Transmit, receive, idle, and sleep power levels in a typical energy model [9].

intelligently switching between the radio's different operation modes. Actually, there are only three modes that a radio can be switched to: transmit mode, active mode (receive, carrier sense and idle modes), and sleep mode. Although further classification of the energy dissipation modes of a radio is possible (*i.e.*, deep/shallow sleep modes, transient modes, *etc.*), the aforementioned classification is detailed enough for the purpose of this study. There is no way to switch between receive, idle, and carrier sense modes: when a node is in the active mode, the actual mode (receive, idle or carrier sensing) is determined by the activities of the node's neighbors, which is not a controllable design parameter. Nevertheless, the ultimate goal is to keep the radio in the sleep mode as long as possible without sacrificing QoS.

The remainder of this paper is organized as follows. Section 2 presents the related work. Section 3 describes the broadcast architectures evaluated in this paper. These broadcast architectures are IEEE 802.11-based flooding, Coordinated Periodic Sleep (CPS)-based flooding, and Multi-Hop Time Reservation using Adaptive Control for Energy efficiency (MH-TRACE)–based flooding. The simulation environment is described in Section 4. Simulation results and analysis for the low traffic regime and high traffic regime are presented in Sections 5 and 6, respectively. We provide a summary of the simulations and analysis in Section 7. Conclusions are drawn in Section 8.

2. Related work

There are several studies that provide a comparative evaluation of network-wide broadcasting and multicasting in mobile ad hoc networks [13–16].

In [13], network layer broadcast protocols for ad hoc networks are categorized into four categories: simple flooding, probability based methods, area based methods, and neighbor knowledge methods. A subset of each category is simulated by using the ns-2 simulator. The simulations are designed to characterize the behavior of protocols under each category. All broadcast architectures in this category utilize IEEE 802.11 as their MAC layer. The performances of the broadcast architectures are characterized in terms of packet delivery ratio, packet delay, and spatial frequency reuse efficiency as functions of traffic load, node density, and node mobility. It is reported in [13] that in a static network the spatial reuse efficiency of probability based and area based methods deteriorate disproportionately with increasing node count, while neighbor knowledge methods approximate the MCDS (Minimum Connected Dominating Set) fairly closely. On the other hand, neighbor knowledge methods that require extended neighbor information do not perform as well in highly mobile networks as they perform in static networks.

In [14], the broadcast storm problem in mobile ad hoc networks is investigated. In this study network layer broadcast schemes are categorized into five categories: probabilistic schemes, counter-based schemes, distance-based schemes, location-based schemes, and cluster-based schemes. The IEEE 802.11 MAC layer is utilized for all the schemes. A comparison of all five schemes is conducted through simulations (the simulator is custom created for this study). The performance metrics used in this study are: reachability (the number of mobile hosts receiving the broadcast message divided by the total number of mobile hosts that are reachable), saved rebroadcasts ($(r - t/r$, where r is the number of hosts receiving the broadcast message, and t is the number of hosts that actually transmitted the message), and average latency (the interval from the time the broadcast was initiated to the time the last host finished its rebroadcasting). The performances of the broadcast schemes are investigated in the network area, node mobility, and traffic load space. It is reported in [14] that as compared to the basic flooding approach, a simple counter-based scheme can eliminate many redundant rebroadcasts when the host distribution is dense. Among the broadcast schemes compared in this study, it is reported that the location-based scheme is the best choice due to its ability to eliminate most redundant rebroadcasts under a wide range of host distributions without compromising reachability.

In [15], a comparative performance study of flooding in ad hoc networks is presented. Five different flooding protocols (flooding with multipoint relay, flooding with active clustering, flooding with passive clustering, flooding with reverse path forwarding, and blind flooding) are evaluated using the GloMoSim simulator. Although not explicitly specified in the paper, it is inferred from the context that the IEEE 802.11 MAC layer is used for all simulations. The performance metrics in this study are the probability of rebroadcast (fraction of nodes that rebroadcast the packet), the ratio of delivered versus expected broadcast packets, and the total control packets in bytes. Node density, traffic load, and mobility level constitute the axis of the sample space. It is reported in [15] that among all the schemes investigated, passive clustering is found to be the most robust scheme for a broad range of mobility and node density values. Similar to the findings of [13], it is found that a scheme that works effectively only with complete neighbor topology information is severely impaired by an increase in node density and mobility level. Furthermore, it is also reported that each scheme investigated has a different set of suitable applications.

In [16], a comparative investigation of algorithms for computing energy-efficient multicast trees in ad hoc wireless networks is presented. Unlike the aforementioned studies, this study is theoretical rather than practical because the network is treated as a static graph and the effects of medium access control, traffic load, and node mobility are not incorporated in the numerical performance evaluation. Furthermore, the only source of energy dissipation is the transmit mode and all the other sources of energy dissipation (*i.e.*, receive, carrier sense, idle, and sleep mode energy dissipations) are ignored.

Our study is different from the aforementioned studies in the following ways. First, in all the previous studies either only a single MAC protocol (IEEE 802.11) is used or no MAC layer is used at all to investigate the performance of different network layer broadcast protocols. However, in this study a single network layer broadcast protocol (flooding) is used to investigate the performance of multiple MAC protocols. Second, our performance metrics to evaluate the broadcast architectures are more extensive than the metrics used in the previous studies. For example, energy dissipation (including all the different components of the energy dissipation) and delay jitter are metrics not considered in the prior work [13–16].

3. Broadcast architectures

In this paper, we evaluate the QoS and energy dissipation characteristics of three flooding based network-wide broadcast architectures (IEEE 802.11-based flooding, CPS-based flooding, and MH-TRACE-based flooding) within the (data rate, node density, network size/topology) parameter space. There are three main reasons for choosing these three MAC protocols to evaluate the performance of flooding: (i) the IEEE 802.11 standard is well known by the wireless community, and almost all researchers compare their algorithms with IEEE 802.11, making it possible to compare CPS and MH-TRACE with any other protocol by just comparing the performance relative to IEEE 802.11, (ii) CPS is a generic energy saving algorithm built on top of IEEE 802.11, and it represents a wide range of energy saving MAC protocols based on CSMA, and (iii) MH-TRACE is a MAC protocol specifically designed for energy-efficient single-hop real-time data dissemination. Furthermore, MH-TRACE is an example of a clustering based approach and a TDMA based channel access scheme. In this section, we provide brief descriptions of these architectures.

3.1. Flooding

Flooding is the simplest broadcasting algorithm, where each node rebroadcasts every packet it receives for the first time. Each node keeps track of the packets it received (*i.e.*, the source node ID and packet sequence number given by the source creates a unique global ID for each packet), and duplicate rebroadcasts are avoided. Furthermore, the sequence ID need not be more than the ratio of the packet drop threshold to the packet generation period in voice broadcasting (*i.e.*, 150/25 ms). Flooding is also a stateless algorithm, so the nodes do not need to create a routing framework (*e.g.*, routing tables, gateways, route caching, etc.).

3.2. IEEE 802.11-based flooding

In broadcasting mode, IEEE 802.11 uses *p*-persistent CSMA with a constant defer window length (*i.e.*, the default minimum defer period) [17,18]. When a node has a packet to broadcast, it picks a random defer time and starts to sense the channel. When the channel is sensed idle, the defer timer counts down from the initially selected defer time at the end of each time slot. When the channel is sensed busy, the defer timer is not decremented. Upon the expiration of the defer timer, the packet is broadcast.

However, when performing network-wide flooding, the contention resolution algorithm of IEEE 802.11 cannot successfully avoid collisions due to the high number of nodes contending for channel access concurrently. One method to avoid this problem is to spread out the packet transmissions at a higher level (*e.g.*, the network layer) by applying a random delay chosen from a uniform distribution between $[0, T_{\text{spread}}]$.

The IEEE 802.11 standard includes an energy saving mechanism when it is utilized in the infrastructure mode. A mobile node that needs to save energy informs the base station of its entry to the energy saving mode, where it cannot receive data (*i.e.*, there is no way to communicate with this node until its sleep timer expires), and switches to the sleep mode. The base station buffers the packets from the network that are destined for the sleeping node. The base station periodically transmits a beacon packet that contains information about such buffered packets. When the sleeping node wakes up, it listens for the beacon from the base station, and upon hearing the beacon responds to the base station, which then forwards the packets that arrived during the sleep period. While this approach saves energy, it is not applicable in ad hoc mode, which we evaluate in this study.

IEEE 802.11 supports an energy saving mechanism in ad hoc mode called ad-hoc traffic indication message (ATIM) window [19]. This mechanism tries to save energy by reducing the time of idle listening, and it does not address the overhearing problem. Furthermore, ATIM is primarily intended for unicast traffic, thus, in broadcasting its energy saving potential is limited.

3.3. CPS-based flooding

Many approaches have been proposed for reducing the energy dissipation of the IEEE 802.11 protocol [20–24]. The basic design philosophy of most of these approaches is letting the nodes sleep periodically in a coordinated fashion to avoid energy dissipation in the idle mode without degrading the system performance. We designed the Coordinated Periodic Sleep (CPS) protocol for broadcasting as a representative of the aforementioned CSMA based energy saving protocols. Actually, we take the basic design philosophy of these approaches, which is letting the nodes sleep periodically to save energy, and modified IEEE 802.11 to create the CPS protocol.

In CPS, time is organized into sleep/active time frames with duration T_{CPS}, which repeat cyclically. Each frame is divided into two periods: (i) the active period with duration T_{active}, where nodes can receive and transmit data, and (ii) the sleep period with duration T_{sleep}, where nodes stay in a low energy sleep state (see Fig. 5). The ratio of the sleep period in each sleep/active cycle, R_{CPS}, is determined according to the QoS requirements of the application. Higher sleep/active ratios will result in higher energy savings at the expense of reduced effective bandwidth (*i.e.*, a reduction of the actual usable time corresponds to an effective reduction of the bandwidth).

In CPS, sleep/active mode switching is synchronized throughout the network (*i.e.*, we assume global synchronization, which is available through the Global Positioning System). In active mode, CPS operation is similar to IEEE 802.11. However, if at the end of an active period a packet is not transmitted, then it is delayed until the sleep period ends, which increases the packet delay when compared to IEEE 802.11.

3.4. MH-TRACE-based flooding

Multi-Hop Time Reservation Using Adaptive Control for Energy Efficiency (MH-TRACE) is a MAC protocol designed for energy-efficient data broadcasting [24]. Fig. 6 shows a snapshot of MH-TRACE clustering and medium access for a portion of a distribution of mobile nodes. In MH-TRACE, the network is partitioned into overlapping clusters through a distributed algorithm. Time is organized into cyclic constant duration superframes consisting of several frames. Each clusterhead chooses the least noisy frame to operate within and dynamically changes its frame according to the interference level of the dynamic network. Nodes gain channel access through a dynamically updated and monitored transmission schedule created by the clusterheads, which eliminates packet collisions within the cluster. Collisions with the members of other clusters are also minimized by the clusterhead's selection of the minimal interference frame.

Ordinary nodes are not static members of clusters, but they choose the cluster they want to join based on the spatial and temporal characteristics of the traffic, taking into account the proximity of the clusterheads and the availability of the data slots within the corresponding cluster. Each frame consists of a control sub-frame for transmission of control packets and a contention-free data sub-frame for data transmission (see Fig. 7). Beacon packets are used for the announcement of the start of a new frame; Clusterhead Announcement (CA) packets are used for reducing co-frame cluster interference; contention slots are used for initial channel access requests; the header packet is used for announcing the data transmission schedule for the current frame; and Information Summarization (IS) packets are used for announcing the upcoming data packets. IS packets are crucial in energy saving. Each scheduled node transmits its data at the reserved data slot.

In MH-TRACE, nodes switch to sleep mode whenever they are not involved in data transmission or reception,

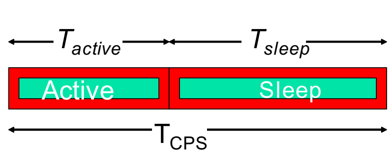

Fig. 5. CPS frame structure.

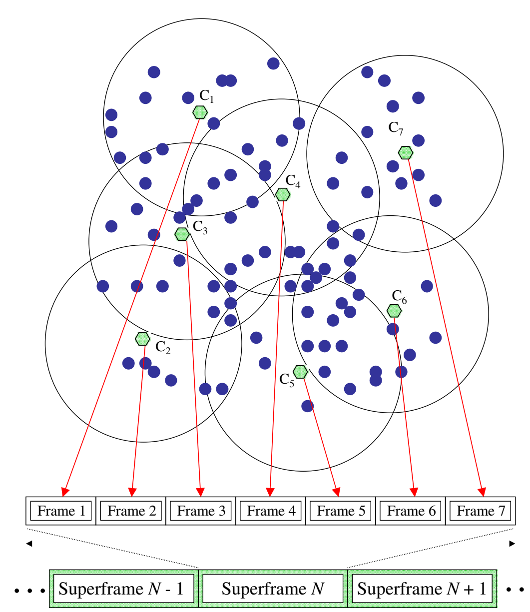

Fig. 6. A snapshot of MH-TRACE clustering and medium access for a portion of an actual distribution of mobile nodes. Nodes C1–C7 are clusterhead nodes.

Please cite this article in press as: B. Tavli, W.B. Heinzelman, QoS and energy efficiency in network wide broadcasting: ..., Comput. Commun. (2007), doi:10.1016/j.comcom.2007.07.005

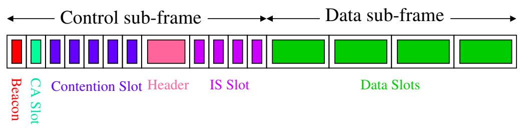

Fig. 7. MH-TRACE frame structure.

which saves the energy that would be wasted in idle mode or in carrier sensing. Ordinary nodes are in the active mode only during the beacon, header, and IS slots. Furthermore, they stay active for the data slots that they are scheduled to transmit or receive. In addition to these slots, clusterheads stay in the active mode during the CA and contention slots.

The source ID and the packet sequence number are embedded into the IS packet, so that nodes that have already received a particular data packet avoid receiving duplicates of the same packet, which saves a considerable amount of energy.

In network wide broadcasting many branches of the broadcast tree consist of multiple hops. Applying a single packet drop threshold in each node is not a good strategy, because of the fact that the packets do not need to be dropped until the packet delay exceeds the packet drop threshold. Due to the network dynamics, packet delay is accumulated in time, and a significant portion of the packets are transmitted by the source node at the verge of being dropped. These packets cannot be relayed and are dropped by the neighbors of the source node. The remedy for this problem is to use two packet drop thresholds. At the source node, a smaller packet drop threshold, $T_{\text{drop-source}}$, is utilized so that packets that cannot be relayed due to large delays do not waste bandwidth and are automatically dropped by the source node. The rest of the nodes in the network use the standard T_{drop}, which is dictated by the application layer. The optimal value of $T_{\text{drop-source}}$ is the superframe time, T_{SF}. This is because $T_{\text{drop-source}}$ should be as low as possible to keep the overall delay as small as possible; and setting $T_{\text{drop-source}}$ lower than T_{SF} will cause a packet drop before the next packet arrival, which results in an unutilized data slot.

4. Simulation environment

We explored the QoS and energy dissipation characteristics of flooding with the IEEE 802.11, CPS, and MH-TRACE MAC protocols through extensive *ns*-2 [25] simulations. *ns*-2 is a widely used simulation tool in wireless network research [26]. A review of wireless network research papers [27] from an ACM symposium based on 151 articles from a five-year-period reported that 76% of the works used network simulation, and of these 44% of the simulations were conducted with *ns*-2 [26]. Although it is known that *ns*-2 has some inaccuracies in modeling the physical layer of wireless networks [28], it is also true that no model is 100% accurate [26]. In a recent study on experimental validation of the *ns*-2 wireless model using simulation, emulation, and real networks [26], it is reported that packet delivery ratios and network topologies are accurately represented in *ns*-2, once the simulation parameters are accurately adjusted.

We investigated the parameter space with traffic load, node density, and network area/topology as the dimensions. We used a continuous bit rate (CBR) traffic generator with a UDP transport agent to simulate a constant rate voice codec. All the simulations were run for 100 s and repeated three times. We used the energy and propagation (two-ray ground) models discussed in [9]. Transmit radius, D_{Tr}, and carrier sense range, D_{CS}, are 250 and 507 m, respectively. Data packet overhead is 10 bytes for IEEE 802.11, CPS, and MH-TRACE. MH-TRACE control packets are 10 bytes, except the header packet, which is 22 bytes. Acronyms, descriptions and values of the constant parameters used in the simulations are provided in Table 1.

We used the random way-point mobility model where the node speeds were chosen from a uniform random distribution between 0.0 and 5.0 m/s (the average pace of a marathon runner). Throughout the simulation time, the average instantaneous node speeds never dropped below 2.3 m/s in any of the scenarios we employed. The pause time is set to zero to avoid non-moving nodes throughout the simulation time. The source node is located in the center of the network. This scenario corresponds to applications where one primary user needs to communicate with all the other users in the network. For example, in a battlefield scenario, the commander of a unit (*i.e.*, a squadron) needs to communicate with all the soldiers currently connected to the network.

Although there are many dimensions in ad hoc networks, we limit our study to node density, traffic load, and network area. Medium access control in ad hoc wireless networks is a relatively easy task when the node density is low and the traffic load is light. However, as the node density and traffic load increase, the performance of the MAC protocols starts to deteriorate. This is because the demand for bandwidth increases with increasing data rate, and the contention for channel access increases with

Table 1
Constant simulation parameters

Var.	Description	Value
C	Channel rate	2 Mbps
D_{Tr}	Transmission/reception range	250 m
D_{CS}	Carrier sense range	507 m
T_{drop}	Packet drop threshold	150 ms
T_{spread}	Spreading delay	12.5 ms
P_T	Transmit power	600 mW
P_R	Receive power	300 mW
P_I	Idle power	100 mW
P_S	Sleep power	10 mW
N/A	Data packet overhead	10 bytes
N/A	Control packet size	10 bytes
N/A	Header packet size	22 bytes
IFS	Inter-frame space	16 μs

Please cite this article in press as: B. Tavli, W.B. Heinzelman, QoS and energy efficiency in network wide broadcasting: ..., Comput. Commun. (2007), doi:10.1016/j.comcom.2007.07.005

increasing node density. Once a certain node density/traffic load point is exceeded, the QoS performance of the network decreases to unacceptable levels. Thus, sampling the performance of a MAC protocol in the node density/traffic load space is very informative to characterize its performance. In broadcast routing of data (*e.g.*, flooding) the average number of hops between the source and destinations is an important factor affecting the QoS performance. The average number of hops between the source and destinations increases with increasing network area, thus, we sampled the network area space to characterize the QoS performance of flooding with different MAC protocols. Furthermore, increasing the network area increases the number of interacting and interfering nodes in the network and hence provides information on the characteristics of the MAC protocols under increasing interference levels.

We examine the traffic load in two regimes: the low traffic regime, which is between 8 and 32 Kbps, and the high traffic regime, which is 32 to 128 Kbps. The sampling in the low traffic regime is denser (8 Kbps steps) when compared to the high traffic regime (32 Kbps steps). Traffic (data rate) is changed by varying the packet size, which is presented in Table 2. The main reason for dividing the traffic axis into two parts is that the CPS protocol can efficiently function only in the low traffic regime. Thus, in the low traffic regime all three of the MAC protocols are evaluated, but in the high traffic regime only IEEE 802.11 and MH-TRACE are evaluated.

Node density is varied between 62.5 nodes per km^2 (40 nodes in an 800 by 800 m area) and 156.25 nodes per km^2 (100 nodes in an 800 by 800 m area) in 31.25 nodes per km^2 steps (see Table 3). Note that the lowest node density (62.5 nodes/km^2) is barely enough to create a connected mobility scenario with the random waypoint model.

Four different network sizes (and topologies) are utilized in the simulations: 800 by 800 m, 800 by 1200 m, 800 by 1600 m, and 800 by 2000 m. We use a rectangle shaped network topology (except the 800 by 800 m network) rather than a square network in order to keep the number of nodes in reasonable limits while increasing the average source/destination path length.

We sampled the traffic-density-area space using eight paths through the parameter space, which we call sampling paths (see Fig. 8). The first sampling path represents the variation of data rate (8–32 Kbps) in the low traffic regime while keeping the area (800×800 m) and density (62.5 nodes/km^2) constant. The second and third sampling paths represent the variation of density (62.5–156.25 nodes/km^2) and area (800×800 m to 800×2000 m), respectively, while keeping traffic (8 Kbps) and either area (800×800 m) or density (62.5 nodes/km^2) constant. The fourth sampling path represents the variation of all parameters, where the network conditions get harsher along the path (see Table 4). The fifth, sixth, seventh, and eight sampling paths are the counterparts of the first, second, third, and fourth sampling paths in the high traffic regime, respectively.

The metrics that we used in this study are average and minimum packet delivery ratios (PDR_{Avg} and PDR_{Min}), packet delay, delay jitter, and energy dissipation. Packet delivery ratio of node i (PDR_i) is the ratio of the total number of data packets received by node i to the number of packets generated by the source node. Average PDR is obtained by averaging the PDRs of all the mobile nodes (N mobile nodes in total)

$$\mathrm{PDR}_{\mathrm{Avg}} = \frac{1}{N}\sum_{k=1}^{N}\mathrm{PDR}_i \tag{1}$$

Minimum PDR is the PDR of the node with least PDR. Average packet delay at node i ($Delay_{\mathrm{Avg}\text{-}i}$) is obtained

Table 2
Data rate and corresponding data packet payload

Regime	Data rate (Kbps)	Payload (Byte)	Packet Gen Period (ms)
	8	50	50.0
	16	50	25.0
Low	24	75	25.0
	32	100	25.0
High	64	200	25.0
	96	300	25.0
	128	400	25.0

Table 3
Number of nodes and node density in an 800×800 m network

Number of nodes	Node density (nodes/km^2)
40	62.5
60	93.75
80	125
100	156.25

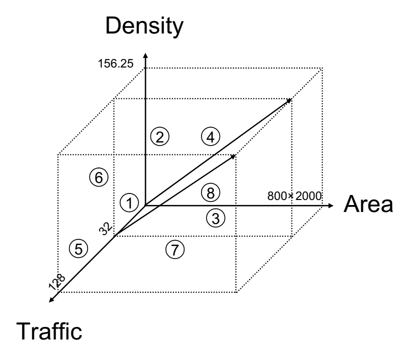

Fig. 8. Sampling the traffic-density-area space.

Table 4
Data rate, node density, and area for 4th and 8th paths

Path	Data rate (Kbps)	Node density (nodes/km^2)	Area (m^2)
	8	62.5	800×800
4	16	93.75	800×1200
	24	125	800×1600
	32	156.25	800×2000
	32	62.5	800×800
8	64	93.75	800×1200
	96	125	800×1600
	128	156.25	800×2000

Please cite this article in press as: B. Tavli, W.B. Heinzelman, QoS and energy efficiency in network wide broadcasting: ..., Comput. Commun. (2007), doi:10.1016/j.comcom.2007.07.005

by averaging the delays (T_j) of all the packets that are received for the first time at node i (M_i), and the global average delay is the average of the delays of N mobile nodes.

$$\mathrm{Delay}_{\mathrm{Avg}} = \frac{1}{N}\sum_{i=1}^{N}\left(\frac{1}{M_i}\sum_{j} T_j\right) \tag{2}$$

RMS delay jitter, which is a measure of the deviation of the packet inter arrival time from the periodicity of the packet generation period, T_{PG}, is obtained by using the following equation:

$$\mathrm{Jitter}_{\mathrm{RMS}} = \sqrt{\frac{1}{N}\sum_{i=1}^{N}\left(\frac{1}{M_i - 1}\sum_{j}\left(T_j - T_{j-1} - T_{\mathrm{PG}}\right)^2\right)} \tag{3}$$

All the energy dissipation results presented in this paper are the time and ensemble averages, and they are expressed in per node per second energy dissipation form with units mJ/s. Both total energy dissipation (Tot E) and the components of the total energy dissipation – transmit (Trn E), receive (Rcv E), carrier sense (CS E), idle (Idl E), and sleep (Slp E) energy dissipations – results are presented to show during which activities the nodes dissipate energy. *ns*-2 is a discrete event simulator, thus, it is possible to keep track of each packet transmission and reception because each packet is a discrete event [23]. Energy dissipation in transmit, receive, and carrier sense modes are calculated by using the durations of packet transmissions and receptions (including collisions and carrier sensing). Idle and sleep mode energy dissipation terms are calculated by keeping track of the total idle and sleep times, respectively, at each node.

Simulation results and analysis are presented in the following two sections.

5. Low traffic regime

5.1. The first sampling path

Data points in the first sampling path are taken along the 8–32 Kbps portion of the traffic axis, where the number of nodes (40 nodes) and network area/topology (800×800 m) is kept constant. IEEE 802.11 performance is summarized in Table 5. In the low traffic regime, both the average and the minimum PDR of IEEE 802.11 is almost perfect due to the low level of congestion. The congestion level of the network increases with the an increase in the traffic, which is indicated by the increasing number of collisions per transmission with the increasing data rate. However, the number of collisions does not reduce the PDR due to the redundancy of flooding in the low traffic regime. Even if a packet reception from one rebroadcast node collides, there are many other redundant versions.

Average packet delay is far from the packet drop threshold; however, we see an increasing trend in the packet delay due to the congestion level of the network. Delay jitter, on the other hand, is stable around 5 ms starting with the 16 Kbps data rate. At 8 Kbps data rate, the jitter, 6 ms, is slightly higher than the rest of the data rates, because of the longer inter-arrival time of the data packets at 8 Kbps (see Table 2). There are no dropped packets in IEEE 802.11 in the low traffic regime.

Table 5
Simulation results for IEEE 802.11 in the first sampling path

	8 K	16 K	24 K	32 K
PDR (avg) (%)	99	99	99	99
PDR (min) (%)	99	99 99	99	
Delay (ms)	8	8	9	10
Jitter (ms)	6	5	5	5
Coll/Trans.	1.7	1.8	2.5	3.1
Tot E/node (mJ/s)	136.2	171.1	198.7	222.3
Trn E/node (mJ/s) (%)	2.9/2.1	5.7/3.3	8.2/4.1	10.4/4.7
Rcv E/node (mJ/s) (%)	19.8/14.6	39.5/23.1	55.4/27.9	69.3/31.2
CS E/node (mJ/s) (%)	29.4/21.6	58.5/34.2	80.9/40.7	99.7/44.9
Idl E/node (mJ/s) (%)	84.1/61.7	67.4/27.3	54.2/27.3	42.9/19.3

Average energy dissipation per node (Tot E) increases by 63.2% from 8 to 32 Kbps due to the increase in transmit (Trn E), receive (Rcv E), and carrier sense (CS E) energy dissipation terms in parallel with the increase in the data rate. At 8 Kbps data rate, 83.3% of the total time is spent in the idle mode, which results in 61.7% of the total energy dissipation, whereas at 32 Kbps, 42.5% of the time is spent in the idle mode and only 19.3% of the energy dissipation is spent in the idle mode due to the reduction in the inactive time (*i.e.*, higher data rates result in higher transmit time percentages, which also increase the receive and carrier sense time percentages). The dominant energy dissipation term is carrier sensing at 32 Kbps data rate, which constitutes 44.9% of the total energy dissipation. Although the percentage of transmit energy dissipation is increasing with the data rate, it is still the smallest energy dissipation term. As expected, the ratio of receive and transmit energy dissipations, 6.8 ± 0.1, is almost constant for all data rates due to the low level of congestion (*i.e.*, receive/transmit ratio is equal to the average number of neighbors in a collision free network).

Simulation results for CPS in the first data path are shown in Table 6. The sleep/active cycle period, T_{CPS}, is matched to the packet generation period, T_{PG}, to avoid the excessive interference and contention of sequential data packet waves from the source node. The sleep/active ratio, R_{CPS}, is adjusted to maximize the sleep time while satisfying the QoS requirements of the voice traffic (*i.e.*, minimum PDR is at least 95%), which is the reason that the minimum PDR stays constant. The reason for the monotonic decrease of R_{CPS} is that the higher R_{CPS} is not maintainable with an increasing congestion level of the network (induced by the increase in the data rates) without sacrificing QoS. Average packet delay of CPS is higher than that of IEEE 802.11 due to the sleep periods, where no packet transmissions take place; however, the delay is still much lower than T_{drop}. Both delay and jitter decrease with increasing data rate due to shorter sleep periods.

Please cite this article in press as: B. Tavli, W.B. Heinzelman, QoS and energy efficiency in network wide broadcasting: ..., Comput. Commun. (2007), doi:10.1016/j.comcom.2007.07.005

Table 6
Simulation results for CPS in the first sampling path

	8 K	16 K	24 K	32 K
PDR (avg) (%)	96	96	96	95
PDR (min) (%)	95	95	95	95
Delay (ms)	20	16	15	12
Jitter (ms)	19	13	12	11
Coll/Trans	4.0	3.9	4.1	4.2
Drop Pck/s	3.4	4.4	6.7	15.5
T_{CPS} (ms)	50.0	25.0	25.0	25.0
R_{CPS}	0.70	0.38	0.25	0.13
Tot E/node (mJ/s)	72.3	136.9	176.2	206.6
Trn E/node (mJ/s) (%)	2.8/3.9	5.6/4.1	8.0/4.6	10.0/4.8
Rcv E/node (mJ/s) (%)	18.3/25.4	36.9/26.9	51.9/29.4	63.0/30.5
CS E/node (mJ/s) (%)	26.4/36.6	53.5/39.1	73.9/42.0	88.1/42.7
Idl E/node (mJ/s) (%)	17.6/24.4	37.1/27.1	39.8/22.6	44.2/21.4
Slp E/node (mJ/s) (%)	7.0/9.8	3.8/2.8	2.5/1.4	1.3/0.6

Table 7
Simulation results for MH-TRACE in the first sampling path

	8 K	16 K	24 K	32 K
PDR (avg) (%)	99	99	99	99
PDR (min) (%)	99	99	99	99
Delay (ms)	44	45	44	43
Jitter (ms)	2	2	2	2
Drop. Pck./s	75	306	332	523
Data Slots/Superframe	70	49	42	35
Tot E/node (mJ/s)	59.9	55.4	54.0	50.8
Trn E/node (mJ/s) (%)	4.6/7.7	5.9/10.9	7.8/14.3	8.2/16.1
Rcv E/node (mJ/s) (%)	11.1/18.7	10.5/19.5	11.9/21.9	11.9/23.4
CS E/node (mJ/s) (%)	12.8/21.5	11.5/21.2	11.1/20.5	8.2/16.1
Idl E/node (mJ/s) (%)	24.4/40.8	18.8/34.8	16.0/29.4	14.7/29.0
Slp E/node (mJ/s) (%)	6.8/11.3	7.4/13.7	7.6/14.0	7.8/15.4

Table 8
MH-TRACE parameters: Number of frames per superframe, N_F, number of data slots per frame, N_D, and data packet payload

Data rate (Kbps)	N_F	N_D	Payload
8	7	10	25 B
16	7	7	50 B
24	7	6	75 B
32	7	5	100 B
64	7	3	200 B
96	7	2	300 B
128	6	2	400 B

Average energy dissipation of CPS at 32 Kbps data rate is 186% more than the energy dissipation at 8 Kbps data rate due to the reduction in sleep time, which is utilized in transmit, receive, carrier sense, and idle modes to cope with the higher data rates. CPS average energy dissipation at 8 Kbps data rate is 47% less than that of IEEE 802.11, which is mainly due to the reduction in the idle energy dissipation (*i.e.*, CPS idle energy dissipation is 20% of the idle energy dissipation of IEEE 802.11 at 8 Kbps data rate). The major energy dissipation term of CPS is the carrier sense energy dissipation, and it is unavoidable, because of the fact that carrier sensing is one of the main building blocks of CSMA type medium access control. Receive energy dissipation is the second largest component of the total energy dissipation, most of which is dissipated on redundant packet receptions. However, in broadcasting it is not possible to discriminate packets due to the lack of RTS/CTS packets. Energy savings of CPS reduces to 7.6% when compared to IEEE 802.11 at 32 Kbps data rate, because of the higher data rate and congestion level of the network. Again, carrier sensing constitutes the largest energy dissipation term and the receive energy dissipation is the second largest energy dissipation term. Transmit energy dissipation never exceeds 5% of the total energy dissipation at any data rate.

MH-TRACE simulation results are presented in Table 7. Due to the TDMA structure of MH-TRACE, the length of the data slots should be changed when the data packet length is changed, which results in a change in the number of data slots in each superframe (*i.e.*, superframe length is kept approximately constant, 25.0 ms, thus, larger size data slots result in lower total data slots within a frame and vice versa). For example, there are total of 70 data slots (10 data slots in each of the 7 frames) with 25-byte payload data packets at 8 Kbps data rate and 35 data slots with 100-byte payload data packets at 32 Kbps data rate (see Table 8).

MH-TRACE average and minimum PDRs are almost perfect at all data rates (*i.e.*, higher than 99%). However, MH-TRACE packet delay is much higher than both IEEE 802.11 and CPS due to its superframe structure, where nodes can transmit at most once in one superframe. On the other hand, MH-TRACE jitter is about 60% less than the jitter of IEEE 802.11 for all data rates, which is as important as the average delay in multimedia applications. Reservation based channel access is the main reason for such low jitter in MH-TRACE. The average number of dropped packets per second is much higher than the other schemes due to the limited number of data slots (*i.e.*, there is a hard limit on the number of nodes that can have channel access, which is common to all TDMA schemes).

A point worth mentioning is that MH-TRACE is fairly sensitive to the mismatches between the packet generation period, T_{PG}, and the superframe time, T_{SF}. For example a 1.5% mismatch between T_{PG} and T_{SF} results in 98% and 97% average and minimum PDRs, respectively, and 22 ms packet delay at 32 Kbps data rate. The reason for such behavior is that a certain percentage of the packets, which is approximately equal to the mismatch percentage, are dropped periodically. This also decreases the overall packet delay. Nevertheless, the PDR loss is not high. The packet generation period and the superframe time are matched for the scenarios we present in this study.

Analysis of MH-TRACE energy dissipation is a complex task due to its detailed energy conservation mechanisms. In MH-TRACE nodes dissipate energy on both data packets and control packets. For example, when there is no data traffic, the per node energy dissipation of MH-TRACE is 31.6 mJ/s with 8 Kbps configuration, which consists of: (i) transmit (11%), receive (6%), and carrier sense (10%) energies dissipated on control packets (*i.e.*, Beacon, Header *etc.*), (ii) idle energy (57%) dissipated during the IS slots (all nodes), and the contention slots (only clusterheads), and (iii) sleep mode energy dissipation (26%). When the data traffic is non-zero, nodes dissipate more energy during the IS slots due to the fact that the IS slots are not silent any more (*i.e.*, IS packets are transmitted) and energy dissipation for receive or carrier sensing is three times the energy dissipation for idling.

All of the nodes remain in the active mode during the IS slots, which is the main source of energy dissipation. There is exactly one IS slot for each data slot, and whether the corresponding data slots are utilized or not, all the nodes listen to the IS slots. Actually, this is the mechanism that enables MH-TRACE to avoid receiving redundant packets. For example, if there are 10 data slots in a frame, there are also 10 IS slots in the same frame, and each node should either be receiving all the packets transmitted in the IS slots, waiting in the idle mode, or dissipating energy on carrier sensing. Therefore, the energy dissipation is less if the number of data slots is less. The benefit of dissipating energy in IS slots is that the nodes that monitored the current frame through the IS slots will receive only the data packets that they have not received before. Thus, they will not dissipate energy on redundant data receptions, idle listening, carrier sensing or collisions. Since there are fewer IS slots in the higher data rates than in lower data rates, energy dissipated in the idle and carrier sense modes are lower in higher data rates, which is the reason that the total energy dissipation decreases with increasing data rates.

MH-TRACE energy dissipation at 8 Kbps is 17% less than the energy dissipation of CPS and 56% less than IEEE 802.11. Despite the fact that CPS spends slightly more time in the sleep mode at 8 Kbps data rate than MH-TRACE, its total energy dissipation is more than MH-TRACE because of the extra energy dissipation of CPS in receive and carrier sensing, where MH-TRACE spends most of its active time in the idle mode (idle power is one third of the carrier sense or receive power). At 32 Kbps, MH-TRACE energy dissipation is less than 25% of both CPS and IEEE 802.11. At 8 Kbps data rate, MH-TRACE transmit energy dissipation is more than 58% higher than both CPS and IEEE 802.11 due to the extra control packet transmissions. However, at 32 Kbps data rate MH-TRACE transmit energy dissipation is about 80% of the other schemes because of the denied channel access attempts (*i.e.*, the number of data slots are fixed and less than the total number of the nodes in the network).

5.2. The second sampling path

The number of nodes is increased from 40 to 100 along second sampling path, and the data rate (8 Kbps) and network area/topology (800×800 m) are kept constant. Simulation results for IEEE 802.11 are presented in Table 9. Average and minimum PDR (99%), packet delay (8 ms), and delay jitter (6 ms), of IEEE 802.11 is constant for all node densities, which shows that the level of congestion can be handled by IEEE 802.11 in the low traffic regime even with dense networks. However, the increasing trend of the average number of collisions per transmissions hints at the increasing congestion level of the network.

IEEE 802.11 total energy dissipation increases with the increasing node density due to the increase in the receive and carrier sense energy dissipation terms, which is the result of a higher number of nodes in each node's receive and carrier sense ranges. The transmit energy dissipation does not increase with node density because of the fact that all of the energy entries are normalized with the number of nodes (*i.e.*, per node energy dissipation, per node transmit energy dissipation, *etc.*).

Simulation results for CPS in the second sampling path are presented in Table 10. We kept the minimum PDR of CPS fixed by varying R_{CPS}, which resulted in shortened sleep periods at higher node densities. Both delay and jitter decrease with the increasing node density due to the shortened sleep period. Nevertheless, the congestion level of the network increases with node density, which manifests itself with the increasing trend in packet drops per second and the average number of data packet collisions per transmission.

Average energy dissipation of CPS is 52% of the energy dissipation of IEEE 802.11 in the 40 node network. This ratio increases to 81% for the 100 node network. The reduction in energy savings is due to the increase in receive, carrier sense, and idle energy dissipation.

Table 9
Simulation results for IEEE 802.11 in the second sampling path

	40	60	80	100
PDR (avg) (%)	99	99	99	99
PDR (min) (%)	99	99	99	99
Delay (ms)	8	8	8	8
Jitter (ms)	6	6	6	6
Coll/Trans.	1.7	4.2	8.3	13.4
Tot E/node (mJ/s)	136.2	146.6	157.4	166.3
Trn E/node (mJ/s) (%)	2.9/2.1	2.9/2.0	2.9/1.8	2.9/1.7
Rcv E/node (mJ/s) (%)	19.8/14.6	24.8/16.9	31.5/20.0	37.5/22.6
CS E/node (mJ/s) (%)	29.4/21.6	40.1/27.3	49.6/31.5	56.9/34.2
Idl E/node (mJ/s) (%)	84.1/61.7	78.9/53.8	73.5/46.7	69.1/41.5

Table 10
Simulation results for CPS in the second sampling path

	40	60	80	100
PDR (avg) (%)	96	96	96	96
PDR (min) (%)	95	95	95	95
Delay (ms)	20	18	16	13
Jitter (ms)	19	11	11	9
Coll/Trans.	4.0	5.6	10.1	14.0
Drop Pck/s	3.4	3.8	4.5	5.3
R_{CPS}	0.70	0.60	0.50	0.40
Tot E/node (mJ/s)	72.3	94.2	115.2	134.8
Trn E/node (mJ/s) (%)	2.8/3.9	2.8/2.9	2.8/2.5	2.8/2.1
Rcv E /node (mJ/s) (%)	18.3 /25.4	23.7/25.9	30.6/26.1	36.9/27.3
CS E/node (mJ/s) (%)	26.4/36.6	37.5/39.6	47.1/41	55.5/41.2
Idl E/node (mJ/s) (%)	17.6/24.4	24.2/25.6	29.6/26	35.6/26.4
Slp E/node (mJ/s) (%)	7.0/9.8	6.0/6.4	5.0/4.4	4.0/3.0

Please cite this article in press as: B. Tavli, W.B. Heinzelman, QoS and energy efficiency in network wide broadcasting: ..., Comput. Commun. (2007), doi:10.1016/j.comcom.2007.07.005

MH-TRACE simulation results in the second sampling path are presented in Table 11. The average and minimum PDR, packet delay and delay jitter of MH-TRACE are almost constant for all node densities. Like in the first sampling path, the average packet delay of MH-TRACE is higher than both IEEE 802.11 and CPS in the second sampling path. The number of dropped packets per second increases with increasing node density due to the fact that the higher number of nodes cannot all gain channel access in denser networks. However, note that this does not affect the PDR, due to the redundancy inherent in the flooding protocol.

Average per node energy dissipation of MH-TRACE is 62.3 ± 2.3 mJ/s for all node densities. Per node transmit energy decreases with node density because the ratio of the data transmissions per node decreases with the node density (*i.e.*, the number of data transmissions do not increase as fast as the node density). Actually, the number of data slots does not change significantly when the network area is kept constant because the number of clusterheads is primarily determined by the network area, and the total number of data slots per clusterhead is constant. However, in low density networks, utilization of the data slots of the outer clusterheads are not as high as the utilization of the inner clusterheads. Thus, the number of data slots in use is higher for denser networks, although the number of data slots is not necessarily higher. Both the actual and the percentage contribution of receive and carrier sense energy dissipations increase, and the contribution of the idle and transmit energy dissipations decrease, due to the decrease in the number of transmissions per node with increasing node density (i.e., utilization of the data slots, especially the data slots in the outer parts of the network, increase with the node density). There is a slow increase in the sleep energy dissipation due to the reduction of the ratio of the clusterheads to total number of nodes, which have more time to sleep (*i.e.*, ordinary nodes do not need to stay in the active mode during the contention slots).

5.3. The third sampling path

Along the third sampling path, network area/topology is varied from 800×800 m to 800×2000 m while keeping the data rate (8 Kbps) and node density (62.5 nodes/km^2) constant. The purpose of this sampling path is to reveal the effects of path length on network performance. Simulation results for IEEE 802.11, CPS, and MH-TRACE are summarized in Table 12. Since energy consumption is not significantly affected from the variations in the path length, we do not include the detailed energy dissipation results in Table 12.

IEEE 802.11 PDR is not affected by the variations in path length in the low traffic regime, and it is stable (around 99%) for the path lengths we investigated in the third sampling path. Packet delay and delay jitter increase linearly with the path length from 8 and 6 ms to 16 and 7 ms, respectively. IEEE 802.11 energy dissipation per node does not change significantly and stabilizes around 140 mJ/s.

After the initial reduction from 0.70 to 0.60, CPS sleep/active ratio stays constant at 0.60. Average packet delay of CPS increases from 20 to 50 ms with increasing average path length while the delay jitter varies from 19 to 30 ms. Energy dissipation of CPS is in parallel with the sleep/active ratio. The behavior of IEEE 802.11 and CPS do not change significantly, except the packet delay and jitter, due to the fact that the delay in these medium access schemes is not high enough to affect PDR with the low level of congestion.

Average PDR of MH-TRACE is above 95% for all network topologies; however, minimum PDR drops below 95% starting with the 800×1600 m network. The reason for such low PDR is the high packet delay of MH-TRACE, which is indicated by the average packet delay in Table 12. The nodes with low PDRs are located far from the source node, which is located at the center of the network. On the other hand, MH-TRACE delay jitter is still less than half

Table 11
Simulation results for MH-TRACE in the second sampling path

	40	60	80	100
PDR (avg) (%)	99	99	99	99
PDR (min) (%)	99	99 99	99	
Delay (ms)	44	46	46	45
Jitter (ms)	2	2	2	2
Drop Pck/s	75	219	663	1292
Tot E/node (mJ/s)	59.9	62.9	64.1	62.6
Trn E/node (mJ/s) (%)	4.6/7.7	4.4/7.0	3.8/5.9	3.2/5.2
Rcv E/node (mJ/s) (%)	11.1/18.7	12.7/20.2	14.5/22.5	14.8/23.7
CS E/node (mJ/s) (%)	12.8/21.5	16.8/26.8	19.0/29.6	19.5/31.2
Idl E/node (mJ/s) (%)	24.4/40.8	22.1/35.2	20.0/31.2	18.0/28.9
Slp E/node (mJ/s) (%)	6.8/11.3	6.8/10.8	6.9/10.8	7.0/11.1

Table 12
Simulation results for IEEE 802.11, CPS, and MH-TRACE in the third sampling path

	800×800	800×1200	800×1600	800×2000
IEEE 802.11				
PDR (avg) (%)	99	99	99	99
PDR (min) (%)	99	99	99	99
Delay (ms)	8	10	12	16
Jitter (ms)	6	6	7	7
Tot E/node (mJ/s)	136.2	141.2	140.4	140.5
CPS				
PDR (avg) (%)	96	96	96	96
PDR (min) (%)	95	95	95	95
Delay (ms)	20	27	41	50
Jitter (ms)	19	20	25	30
R_{CPS}	0.70	0.60	0.60	0.60
Tot E/node (mJ/s)	72.3	87.6	87.8	88.2
MH-TRACE				
PDR (avg) (%)	99	99	99	97
PDR (min) (%)	99	99	92	67
Delay (ms)	44	54	73	89
Jitter (ms)	2	2	3	3
Tot E/node (mJ/s)	59.9	62.0	60.8	60.5

Please cite this article in press as: B. Tavli, W.B. Heinzelman, QoS and energy efficiency in network wide broadcasting: ..., Comput. Commun. (2007), doi:10.1016/j.comcom.2007.07.005

of the delay jitter obtained with IEEE 802.11 and is about 10% of CPS delay jitter. MH-TRACE energy dissipation per node stays in a narrow band around 60 mJ/s, which is 63% less than the IEEE 802.11 energy dissipation and 32% less than the CPS energy dissipation for the 800×2000 m network.

5.4. The fourth sampling path

Data points in the fourth sampling path are taken along the diagonal of the low traffic regime parameter space, where *Si* stands for the samples on the path (*i.e.*, the first row of Table 4 is *S*1, the second row of Table 4 is *S*2, and so on). Simulation results obtained along the fourth sampling path for IEEE 802.11, CPS, and MH-TRACE are presented in Table 13.

Average and minimum PDRs of IEEE 802.11 drop below 95% starting with *S*3, because of the high congestion level of the network. Packet delay and jitter also increase along the sampling path. Node density and data rate are the dominant factors affecting the congestion level of the network. Although IEEE 802.11 does not exhibit a significant QoS deterioration in low density and high data rate networks (*i.e.*, *S*1) or high density and low data rate networks (*i.e.*,*S*2), when we combine high node density and high data rate, the resultant congestion level of the network is more than that can be handled by the contention resolution mechanism of IEEE 802.11. Energy dissipation of IEEE 802.11 increases along the sampling path due to the increase in the total number (node density) and size (data rate) of data packet transmissions.

Since the performance of IEEE 802.11 is below the QoS requirements for the second half of the fourth sampling path, it is not meaningful to try to save energy, which would further deteriorate the QoS. Thus, CPS results are presented only for the first half of the fourth sampling path. The sleep/active ratio of CPS drops from 0.70 at *S*1 to 0.28 at *S*2. CPS energy dissipation is 10% less than that of IEEE 802.11 at *S*2.

Surprisingly, MH-TRACE minimum PDR is above 95% all along the fourth sampling path, unlike the third sampling path, where MH-TRACE minimum PDR drops below 95% in the second half of the third sampling path. By investigating the paths traversed by the packets, we found that the average number of hops from the source to the mobile nodes decreases with node density due to the increase in connectivity (*i.e.*, average degree of a node). MH-TRACE packet delay at highly congested networks is comparable with the packet delay of IEEE 802.11 (*i.e.*, MH-TRACE packet delay is 50% more than IEEE 802.11 packet delay at *S*4), while IEEE 802.11 packet delay is significantly lower than MH-TRACE delay at lightly loaded networks (*i.e.*, IEEE 802.11 packet delay at *S*1 is less than 20% of MH-TRACE packet delay).

The decrease in the per node energy dissipation of MH-TRACE is mainly due to the increase in node density and decrease in the number of data slots, which are explained in detail in Section 5.1. MH-TRACE energy dissipation is less than a third of the energy dissipation of CPS at *S*2, and at *S*4 MH-TRACE energy dissipation is less than a fifth of the energy dissipation of IEEE 802.11.

Table 13
Simulation results for IEEE 802.11, CPS, and MH-TRACE in the fourth sampling path

	S1	S2	S3	S4
IEEE 802.11				
PDR (avg) (%)	99	99	92	80
PDR (min) (%)	99	99	91	76
Delay (ms)	8	11	33	58
Jitter (ms)	6	6	12	15
Tot E/node (mJ/s)	136.2	192.9	251.3	292.0
CPS				
PDR (avg) (%)	96	96		
PDR (min) (%)	95	95		
Delay (ms)	20	17		
Jitter (ms)	19	11		
R_{CPS}	0.70	0.28		
Tot E/node (mJ/s)	72.3	173.4		
MH-TRACE				
PDR (avg) (%)	99	99	99	98
PDR (min) (%)	99	99	97	96
Delay (ms)	44	65	77	88
Jitter (ms)	2	2	3	3
Tot E/node (mJ/s)	59.9	56.9	54.3	53.1

6. High traffic regime

Having completed the analysis of the sampling paths within the low traffic regime, starting with the fifth sampling path we focus on the high traffic regime. In the high traffic regime we investigate IEEE 802.11 and MH-TRACE only, because beyond the 32 Kbps data rate it is not possible to save any energy with CPS, which is its main feature.

6.1. The fifth sampling path

Data points in the fifth sampling path are taken along the 32–128 Kbps portion of the traffic axis with the number of nodes (40 nodes) and network area/topology (800×800 m) kept constant. Unlike the first sampling path, where IEEE 802.11 PDR stays constant at 99%, both the average and minimum PDR of IEEE 802.11 drops with increasing data rate (see Table 14) due to severe congestion. Note that despite the fact that the PDR decreases with increasing data rate, throughput (*i.e.*, number of bytes) increases with the increasing data rate. For example, the amount of data relayed to the minimum PDR node at 32 Kbps node is 4 Kbytes per second, whereas at 128 Kbps data rate the amount of data conveyed to the minimum PDR node is 6.25 Kbytes per second. The decrease in the average number of collisions per transmission is due to the decrease in the number of data packet transmissions. Despite the fact that the number of data transmissions decreases with increasing data rate, transmit, receive, and

Please cite this article in press as: B. Tavli, W.B. Heinzelman, QoS and energy efficiency in network wide broadcasting: ..., Comput. Commun. (2007), doi:10.1016/j.comcom.2007.07.005

Table 14
Simulation results for IEEE 802.11 and MH-TRACE in the fifth sampling path

	32 K	64 K	96 K	128 K
IEEE 802.11				
PDR (avg) (%)	99	89	82	78
PDR (min) (%)	99	89	64	39
Delay (ms)	10	31	54	68
Jitter (ms)	5	15	20	22
Coll/Trans	3.1	7.3	6.7	5.5
Drop Pck/s	0.0	9.3	250.2	388.3
Tot E/node (mJ/s)	222.3	273.6	284.5	289.7
MH-TRACE				
PDR (avg) (%)	99	99	99	99
PDR (min) (%)	99	99	93	89
Delay (ms)	43	44	45	44
Jitter (ms)	2	2	2	2
Drop Pck/s	523	907	1234	1199
Tot E/node (mJ/s)	50.8	48.8	45.4	44.4

carrier sense energies increase due to the increase in the size of the data packets.

MH-TRACE average PDR stays constant at 99% in the fifth data path (see Table 14). However, minimum PDR drops below 95% for data rates higher than 64 Kbps. A relatively low number of data slots per superframe is the reason for the low minimum PDR at higher data rates. Since the network layer algorithm is flooding, there is no coordination in relaying the data packets (*i.e.*, statistical multiplexing). When the number of rebroadcasts is low (limited number of data slots per superframe) failure of the formation of a dominating set in some broadcast waves is inevitable. Since the average number of clusterheads is constant for all data rates (*i.e.*, average number of clusterheads is mainly determined by the network size), the number of data slots in the network is determined by the number of data slots per frame (*i.e.*, total number of available data slots in the network is the product of the number of clusterheads and the number of data slots per frame). Thus, some of the nodes, especially the ones far from the source node, have relatively low PDR compared with the rest of the network.

MH-TRACE packet delay and jitter do not change significantly along the fifth sampling path. MH-TRACE energy dissipation exhibits a slight decrease along the fifth sampling path due to the decrease in the number of IS slots, as was described in Section 5.2. MH-TRACE energy dissipation is less than one sixth of the energy dissipation of IEEE 802.11 at 128 Kbps data rate.

Actually, the PDR of IEEE 802.11 is higher in highly congested networks (>64 Kbps) if there is a hard constraint on the maximum packet delay (*i.e.*, packets with delays higher than T_{drop}). Table 15 presents the simulation results for IEEE 802.11 and MH-TRACE along the fifth sampling path with no packet drop threshold (*i.e.*, $T_{\text{drop}} \to \infty$). At 96 and 128 Kbps data rates, average PDR of IEEE 802.11 with packet drops is larger than the case with no packet drops, yet the minimum PDR is higher without packet drops. This is because the average PDR is primarily affected by the congestion level of the network and the difference between the average and minimum PDRs is due to the delay constraint. MH-TRACE PDR is not affected significantly by the packet drop threshold. However, the packet delay rises to formidably high levels, yet, still is a magnitude lower than the IEEE 802.11 packet delay in high congestion (data rate >64 Kbps).

Table 15
Simulation results for IEEE 802.11 and MH-TRACE in the fifth sampling path with $T_{\text{drop}} \to \infty$

	32 K	64 K	96 K	128 K
IEEE 802.11				
PDR (avg) (%)	99	88	74	59
PDR (min) (%)	99	88	73	59
Delay (ms)	10	31	1798	3152
Jitter (ms)	5	15	23	29
Tot E/node (mJ/s)	222.3	273.6	284.5	289.7
MH-TRACE				
PDR (avg) (%)	99	99	99	99
PDR (min) (%)	99	99	99	89
Delay (ms)	191	226	285	312
Jitter (ms)	2	2	3	3
Tot E/node (mJ/s)	50.8	48.8	45.4	44.4

6.2. The sixth sampling path

The number of nodes is increased along the sixth sampling path, while keeping the data rate (32 Kbps) and network area (800×800 m) constant. Table 16 presents the simulation results for IEEE 802.11 and MH-TRACE. IEEE 802.11 average PDR drops below 95% starting with the 60 node network, and reaches 77% for the 100 node network. Decrease of the PDR and increase of the packet delay and delay jitter are all due to the increase in the congestion level of the network with increasing node density. There is not a significant gap between the average and minimum PDRs of IEEE 802.11 due to the comparatively lower packet delays when compared to the packet delays along the fifth sampling path.

Table 16
Simulation results for IEEE 802.11 and MH-TRACE in the sixth sampling path

	40	60	80	100
IEEE 802.11				
PDR (avg) (%)	99	94	88	77
PDR (min) (%)	99	91	88	77
Delay (ms)	10	17	28	33
Jitter (ms)	5	7	13	15
Tot E/node (mJ/s)	222.3	240.4	246.5	247.8
MH-TRACE				
PDR (avg) (%)	99	99	99	99
PDR (min) (%)	99	99	99	99
Delay (ms)	43	41	44	42
Jitter (ms)	2	2	2	2
Tot E/node (mJ/s)	50.8	51.4	50.7	49.9

Please cite this article in press as: B. Tavli, W.B. Heinzelman, QoS and energy efficiency in network wide broadcasting: ..., Comput. Commun. (2007), doi:10.1016/j.comcom.2007.07.005

Both the average and minimum PDR of MH-TRACE stay constant at 99%, and the packet delay also lies in a narrow band around 43 ms. MH-TRACE energy dissipation at 156.25 nodes/km^2 node density is approximately one fifth of the energy dissipation of IEEE 802.11.

6.3. The seventh sampling path

Data points along the seventh sampling path are taken by varying the network size from 800×800 m to 800×2000 m, while keeping the data rate (32 Kbps) and node density (62.5 nodes/km^2) constant. IEEE 802.11 PDR stays above 99% all along the seventh sampling path (Table 17). However, the increase in average packet delay shows that the PDR will start to decrease for longer path lengths. MH-TRACE minimum PDR also drops below 95% in the second half of the sampling path due to the packet drops arising because of the longer paths between the source and the distant nodes. MH-TRACE average and minimum PDRs in the seventh sampling path are lower than their counterparts in the third sampling path because of the fact that the total number of data slots in the higher data rate networks is lower than total number of data slots in the lower data rate networks, which deteriorates the path diversity and consequently increases the packet delay.

6.4. The eighth sampling path

Data points in the eighth sampling path are taken along the diagonal of the high traffic regime parameter space, where *Si* stand for the samples on the path (see Table 4). Simulation results obtained along the eighth sampling path for IEEE 802.11 and MH-TRACE are presented in Table 18. In the eight sampling path, which is the most challenging in this study, both IEEE 802.11 and MH-TRACE failed to maintain a minimum PDR of 95% after the first sample on the path. Congestion is the main reason for such deterioration of IEEE 802.11 due to the increase in the data rate and node density, which means a higher number of larger data packets. The main reason for the deterioration of MH-TRACE performance is the high packet delays due to the increase in average path length and the reduction of the total number of data slots per km^2 along the eighth sampling path. Although the average PDR of MH-TRACE is higher than IEEE 802.11 along the eighth sampling path, the minimum PDR of MH-TRACE is lower than that of IEEE 802.11 at the fourth sampling point due to the excessive packet drops at locations close to the edges of the network. Furthermore, IEEE 802.11 delay is higher than that of MH-TRACE at the fourth sampling point due to the high level of congestion.

We present a summary of all of these simulations and analysis in the following section.

Table 17
Simulation results for IEEE 802.11 and MH-TRACE in the seventh sampling path

	800 × 800	800 × 1200	800 × 1600	800 × 2000
IEEE 802.11				
PDR (avg) (%)	99	99	99	99
PDR (min) (%)	99	99	99	98
Delay (ms)	10	19	33	58
Jitter (ms)	5	8	11	15
Tot E/node (mJ/s)	222.3	235.4	251.3	252.8
MH-TRACE				
PDR (avg) (%)	99	99	88	88
PDR (min) (%)	99	99	40	26
Delay (ms)	43	52	71	86
Jitter (ms)	2	2	3	4
Tot E/node (mJ/s)	50.8	52.5	52.9	53.4

Table 18
Simulation results for IEEE 802.11 and MH-TRACE in the eighth sampling path

	S5	S6	S7	S8
IEEE 802.11				
PDR (avg) (%)	99	88	74	64
PDR (min) (%)	99	76	35	33
Delay (ms)	10	90	98	116
Jitter (ms)	6	24	23	24
Tot E/node (mJ/s)	222.3	272.3	281.2	267.5
MH-TRACE				
PDR (avg) (%)	99	98	90	84
PDR (min) (%)	99	90	40	15
Delay (ms)	43	71	90	106
Jitter (ms)	2	2	2	2
Tot E/node (mJ/s)	50.8	49.6	41.8	46.2

7. Summary

In this paper we investigated the role of medium access control on the QoS and energy dissipation characteristics of network wide real-time data broadcasting through flooding using three MAC protocols (IEEE 802.11, CPS, and MH-TRACE) within the data rate, node density, and network area/topology parameter space. The ranges of the parameter space were chosen to characterize the behavior of the broadcast architectures. Thus, we identified the breaking points of each MAC layer in flooding.

IEEE 802.11 achieves almost perfect PDR in low density networks (where the number of nodes is barely enough to create a connected network with the random waypoint mobility model with pedestrian speed) with low (8 Kbps) to medium (32 Kbps) data rates. However, for higher data rates (*i.e.*, data rates higher than 32 Kbps), IEEE 802.11 PDR exhibits a sharp decrease due to the high level of congestion. In low data traffic networks (8 Kbps), IEEE 802.11 is capable of handling low (62.5 nodes/km^2) to high (156.25 nodes/km^2) node densities without sacrificing the PDR. For high data rates (>32 Kbps), even with low node density IEEE 802.11 cannot maintain network stability, and PDR deteriorates significantly. IEEE 802.11 is virtually immune to changes in the average path length (*i.e.*, for the path

Please cite this article in press as: B. Tavli, W.B. Heinzelman, QoS and energy efficiency in network wide broadcasting: ..., Comput. Commun. (2007), doi:10.1016/j.comcom.2007.07.005

lengths we considered in this study) for low node densities and low data rates because of its relatively lower packet delay. However, there is a limit on the serviceable maximum path length, which is determined by the delay limit of the application (*i.e.*, T_{drop}). IEEE 802.11 performance is affected seriously by the combined high node density and high data rates, which also limits the path length scalability of IEEE 802.11. Energy dissipation of IEEE 802.11 is determined mainly by the total number of packets transmitted, and there is no built-in energy saving mechanisms for IEEE 802.11 in the ad hoc mode of operation.

The main advantage of CPS is its capability of saving energy wasted in the idle mode by the underlying IEEE 802.11 protocol. CPS successfully saves energy in low node density and low data traffic networks without sacrificing the QoS requirements of the application. However, with increasing node densities and/or data rates, CPS energy savings diminishes quickly. For medium node density and low data rate networks, CPS energy savings are only marginal due to the limited sleep time. The same applies to low node density and medium data rate networks for CPS. Although CPS packet delay and delay jitter are higher than IEEE 802.11, it can successfully meet the QoS requirements of the application for longer path lengths in low node density and low data rate networks. CPS cannot operate effectively in the high data regime (>32 Kbps), because the underlying IEEE 802.11 needs all the bandwidth available to avoid congestion; thus, there is no bandwidth available to waste in the sleep mode to save energy.

MH-TRACE can maintain 99% PDR up to medium-high (64 Kbps) data rates in low density networks. Under all node densities with low (8 Kbps) and medium (32 Kbps) data rates, MH-TRACE is capable of maintaining the QoS requirements of the application due to its coordinated channel access mechanism. However, due to its high packet delay, MH-TRACE cannot maintain the required minimum PDR in large networks. However, in combined difficulty levels (low-medium node densities and data rates) MH-TRACE QoS metrics are better than the other schemes. MH-TRACE energy dissipation is significantly lower than the other schemes for the entire parameter space due to its schedule based channel access and data discrimination mechanisms.

8. Conclusions

Having summarized the results of our analysis, we will outline the results and contributions of this study:

(1) IEEE 802.11-based flooding provides satisfactory QoS to real-time data broadcasting in low to medium data traffic and node densities. Furthermore, the scalability of IEEE 802.11 in mild network conditions in terms of path length is better than the other schemes due to its low packet delay. However, under heavy network conditions (high node density and data rate), IEEE 802.11 QoS performance deteriorates sharply, and its scalability is also affected significantly. The energy dissipation of IEEE 802.11 is the highest among all schemes tested. Delay jitter of IEEE 802.11 is lower than CPS and higher than MH-TRACE.

(2) CPS-based flooding sleep ratio shows a steep descent when the network conditions gets harsher. Furthermore, CPS delay jitter is higher than IEEE 802.11 and MH-TRACE. CPS can provide energy efficiency only in low node density and low data traffic networks. Yet, the scalability of CPS is better than MH-TRACE and worse than IEEE 802.11 in such networks. However, it is not possible to employ CPS efficiently in either high density or high data traffic networks. The main reason for such behavior is the CPS energy saving mechanism, which reduces the energy dissipation by reducing the effective bandwidth. On the other hand, when the data rate is very low (*i.e.*, less than 8 Kbps) CPS energy savings outperform MH-TRACE.

(3) MH-TRACE-based flooding provides high energy efficiency to the nodes in the network by its coordinated medium access and data discrimination mechanisms. Especially in high data rate and/or high node density networks, the energy dissipation of MH-TRACE is less than 25% percent of the other schemes. Furthermore, under heavily congested networks, MH-TRACE provides satisfactory QoS to real-time data broadcasting, where the other schemes fail to fulfill the QoS requirements of the application. However, MH-TRACE packet delay performance is not as good as the other schemes, especially in mild network conditions. On the other hand, MH-TRACE packet jitter is lower than the other schemes (*e.g.*, MH-TRACE jitter is less than 10% of the IEEE 802.11 jitter at the eighth sampling path), which is as important as packet delay in multimedia applications.

(4) Data packet discrimination through information summarization is shown to be a very effective method to save energy in network wide broadcasting through flooding, where redundant data retransmissions are unavoidable. Since each packet can be identified by its unique data packet ID, information summarization is not an ambiguous task (*i.e.*, the unique ID of each data packet is sufficient to discriminate the broadcast packets).

(5) Utilization of multiple levels of packet drop thresholds significantly improves the broadcast performance in TDMA based schemes (*e.g.*, MH-TRACE). Furthermore, mismatches between the superframe time and the packet generation period are shown to deteriorate the PDR while improving the packet delay.

(6) The dominant energy dissipation term for a non-energy saving protocol (*e.g.*, IEEE 802.11) in low data traffic and low node density networks is idle lis-

tening. On the other hand, in heavily congested networks, the dominant energy dissipation term is carrier sensing. Although periodic sleep/awake cycling based CSMA-type medium access (*e.g.*, CPS) can save a significant amount of energy by reducing the idle mode energy dissipation, in highly congested networks such energy saving mechanisms cannot provide satisfactory performance. Medium access control based on explicit coordination (*e.g.*, MH-TRACE) is the only option for energy savings in highly loaded networks.

(7) The contribution of transmit energy dissipation is a minor component of the total energy dissipation in the medium access schemes. However, receive mode energy dissipation and carrier sense energy dissipation, which constitute a significant portion of the total energy dissipation, are directly related with the transmit energy dissipation. Thus, we conjecture that the impact of energy saving mechanisms targeted at minimizing the idle mode energy dissipation for mild network conditions and receive and carrier sense energy for heavy network conditions is more than the impact of mechanisms targeted to minimize the transmit energy dissipation only, especially in broadcast scenarios.

References

[1] A.S. Tanenbaum, Computer Networks, Prentice Hall, 2003.
[2] W. Stallings, Wireless Communications and Networks, Prentice Hall, 2002.
[3] J. Janssen, D.D. Vleeschauwer, G.H. Petit, R. Windey, J.M. Leroy, Delay bounds for voice over ip calls transported over satellite access links, ACM/Baltzer Mobile Networks and Applications Journal 7 (2002) 79–89.
[4] ITU-T Recommendation G.711, Pulse Code Modulation (PCM) of Voice Frequencies, ITU, 1988.
[5] ITU-T Recommendation G.726, 40, 32, 24, 16 kbit/s Adaptive Differential Pulse Code Modulation (ADPCM), ITU, 1990.
[6] ITU-T Recommendation G.723.1, Speech Coders: Dual Rate Speech Coder for Multimedia Communications Transmitting at 5.3 and 6.3 kbit/s, ITU, 1996.
[7] ITU-T Recommendation G.131, Control of Talker Echo, ITU, 1996.
[8] ITU-T Recommendation G.114, One Way Transmission Time, ITU, 1996.
[9] W.B. Heinzelman, Application-specific protocol architectures for wireless networks, Ph.D. Dissertation, MIT, Cambridge, MA, 2000.
[10] I.F. Akyildiz, W. Su, Y. Sankarasubramaniam, E. Cayirci, A survey on sensor networks, IEEE Communications Magazine 40 (2002) 102–114.
[11] E.D. Jensen, C.D. Locks, H. Tokuda, A time-driven scheduling model for real systems, in: Proceedings of the IEEE Real Time Systems Symposium, 1985, pp. 112–122.
[12] S. Biswas, S. Datta, Reducing overhearing energy in 802.11 networks by low-power interface idling, in: Proceedings of the IEEE International Conference on Performance, Computing, and Communications, 2004, pp. 695–700.
[13] B. Williams, T. Camp, Comparison of broadcasting techniques for mobile ad hoc networks, in: Proceedings of the ACM International Symposium on Mobile Ad Hoc Networking and Computing (MOBIHOC), 2002, pp. 194–205.
[14] Y-C Tseng, S.Y. Ni, Y.S. Chen, J.P. Sheu, The broadcast storm problem in a mobile ad hoc network, ACM/Kluwer Wireless Networks Journal 8 (2002) 153–167.
[15] Y. Yi, M. Gerla, T.J. Kwon, Efficient flooding in ad hoc networks: a comparative performance study, in: Proceedings of the IEEE International Conference on Communications (ICC), 2003, pp. 1059–163.
[16] S. Athanassopoulos, I. Caragiannis, C. Kaklamania, P. Kanellopoulos, Experimental comparison of algorithms for energy-efficient multicasting in ad hoc networks, Lecture Notes in Computer Science 3158 (2004) 183–196.
[17] B. O'Hara, A. Petrick, The IEEE 802.11 Handbook: A Designer's Companion, IEEE Press, 1999.
[18] T. Cooklev, Wireless Communication Standards, IEEE Press, 2004.
[19] L.M. Feeney, An asynchronous power save protocol for wireless ad hoc networks, Swedish Institute of Computer Science Technical Report SICS-T-2002/9-SE, 2002.
[20] W. Ye, J. Heidemann, D. Estrin, Medium access control with coordinated adaptive sleeping for wireless sensor networks, IEEE/ACM Transactions on Networking 12 (2004) 493–506.
[21] C.S.R. Murthy, B.S. Manoj, Ad Hoc Wireless Networks: Architectures and Protocols, Prentice Hall, 2004.
[22] S. Basagni, M. Conti, S. Giordano, I. Stojmenovic, Mobile Ad Hoc Networking, John Wiley and Sons, 2004.
[23] C.S. Raghavendra, K.M. Sivalingam, T. Znati, Wireless Sensor Networks, Kluwer Academic Publishers, 2004.
[24] B. Tavli, W.B. Heinzelman, Mobile Ad Hoc Networks: Energy-Efficient Real-Time Group Communications, Springer Verlag, 2006.
[25] The Network Simulator ns-2, http://www.isi.edu/nsnam/ns/.
[26] S. Ivanov, A. Herms, G. Lukas, Experimental validation of the ns-2 wireless model using simulation, emulation, and real network, in: Proceedings of the 4th Workshop on Mobile Ad-Hoc Networks (WMAN'07), VDE Verlag, ISBN 978-3-8007-2980-7, 2007, pp. 433–444.
[27] S. Kurkowski, T. Camp, M. Colagrosso, MANET simulation studies: the incredibles, ACM SIGMOBILE Mobile Computing and Communications Review 9 (2005) 50–61. Q1
[28] D. Kotz, C. Newport, R.S. Gray J. Liu, Y. Yuan, C. Elliott, Experimental evaluation of wireless simulation assumptions, in: Proceedings of the ACM International Symposium on Modeling, Analysis, and Simulation of Wireless and Mobile Systems, 2004, pp. 78–82.